Understanding the Impact of Packet Size on the Energy Efficiency of LoRaWAN

Lluís Casals, Carles Gomez, and Rafael Vidal

***Abstract*—LoRaWAN has become a flagship LPWAN technology, and one of the main connectivity alternatives for IoT devices. Since LoRaWAN was designed for low energy consumption, it is fundamental to understand its energy performance. In this paper, we study the impact of packet size on LoRaWAN device energy consumption per delivered data bit (EPB). By means of extensive simulations, we show that, when network performance is very high or very low, EPB decreases steadily with packet size; otherwise, EPB may show an "asymmetric U" shape as a function of packet size, with a minimum EPB value that is achieved for a medium packet size. We also provide detailed insights on the reasons that produce the observed behaviors.**

***Index Terms*—Energy efficiency, IoT, LoRa, LoRaWAN, packet size, PDR.**

I. Introduction

LoRaWAN has become a flagship low power wide area network (LPWAN) technology, and also a popular solution to provide connectivity for Internet of things (IoT) devices [1]–[3]. In 2020, there were already ∼191 million deployed LoRaWAN devices, with recent estimates predicting a rise up to 731 million in 2023 [4]. The advantages of LoRaWAN include low cost –partly thanks to the use of unlicensed frequency bands–, a link range up to several kilometers, low power consumption, and an open network model.

IoT devices (e.g., sensor nodes) often exhibit energy availability constraints, since in many cases they are powered by simple batteries or limited energy-harvesting mechanisms [5]. Therefore, optimizing the energy performance of LoRaWAN devices is crucial.

Several research works have focused on the energy performance of LoRaWAN [6]–[20]. However, to our best knowledge, the influence of LoRaWAN packet size on device energy efficiency has not been sufficiently considered at the time of writing. In this paper, by means of extensive simulations, we focus on the impact of packet size on LoRaWAN device energy consumption per delivered bit (EPB), in a variety of scenarios. We find that, when network performance is very high or very low, the most energy-efficient packet size is the largest one supported for the physical layer data rate (DR) being used; otherwise, a shorter packet size may minimize EPB. In general, the curve that depicts EPB as a function of packet size exhibits an "asymmetric U" shape: A very small packet size incurs high energy overhead per delivered data bit, whereas a large packet size increases the probability of collision and packet drops (and, for confirmed traffic, the number of retransmissions) at the sender. However, the rightmost side of the "asymmetric U" shape will tend to fall outside of the range of valid packet sizes as the network approaches ideal performance or as it becomes impractical. We illustrate the observed EPB behaviors, and provide detailed insights on the reasons that produce them, in a range of scenarios. We believe that our findings will be useful for developers, researchers, engineers, network operators and practitioners in the field of LoRaWAN networks.

The remainder of the paper is organized as follows. Section II provides a technical overview of the LoRaWAN technology. Section III reviews literature work on LoRaWAN energy performance and its relationship with packet size. Section IV evaluates EPB as a function of the LoRaWAN packet size in a wide range of scenarios. Section V discusses the main findings from the evaluation, and assesses the potential impact of further parameters and scenarios on network performance. Finally, Section VI concludes the paper.

II. Technical Overview of LoRaWAN

In this section, we provide a technical overview of LoRaWAN, with a focus on the LoRaWAN characteristics that are most relevant to this article. First, we describe the LoRaWAN network and its protocol architecture. Then, we present the main features of the two fundamental LoRaWAN layers (i.e., the physical layer and the MAC layer).

A. LoRaWAN Architecture

A LoRaWAN network comprises three main types of elements: End-devices (EDs), gateways, and a network server (NS). The ED role has been conceived for IoT devices (e.g., sensors). The LoRaWAN architecture has been designed to centralize at the NS the collection of messages transmitted by EDs. To this end, messages sent by EDs may be received by one or several gateways which then forward the messages to the NS. The communication direction from an ED to the NS is called uplink, whereas the opposite direction is called downlink.

Communication over the radio link between an ED and a gateway is performed by using the LoRaWAN physical layer, whereas message transmission between a gateway and the NS is carried out over an IP-based network [10]. On top of these

Manuscript received March 2, 2023; revised June 27, 2023; approved for publication by Ali Abedi, Division 3 Editor, August 19, 2023.

This work was supported in part by the Spanish Government through project TEC2016-79988-P funded by AEI/FSE/EU, grant PID2019-106808RA-I00 funded by MCIN/AEI/10.13039/501100011033, and by Secretaria d'Universitats i Recerca del departament d'Empresa i Coneixement de la Generalitat de Catalunya with the grant number 2021 SGR 00330.

The authors are with the Department of Network Engineering, Universitat Politècnica de Catalunya, 08860, Castelldefels, Spain. email: {lluis.casals, carles.gomez, rafael.vidal}@upc.edu.

L. Casals is the corresponding author.

Digital Object Identifier: 10.23919/JCN.2023.000039

1229-2370/23/$10.00 © 2023 KICS

two message bearers, the LoRaWAN MAC protocol operates at the EDs and the NS, providing MAC layer functionality. An application runs directly over the LoRaWAN MAC layer.

There are three classes of LoRaWAN devices, in terms of their supported functionality at the physical and MAC layers: Class A, Class B, and Class C. Class A, which is intended for simple and energy-efficient operation, must be implemented by all LoRaWAN EDs. Instead, Class B (which is energy efficient, but with greater complexity) and Class C (intended for EDs without energy constraints) are optional. In consequence, most deployed LoRaWAN networks and research studies on LoRaWAN are based on Class A [2]. Accordingly, in this paper we assume Class A-based LoRaWAN operation. In the next two subsections, we describe the main characteristics of the Class A LoRaWAN physical layer and the MAC layer, respectively.

B. LoRaWAN Physical Layer

The LoRaWAN physical layer offers two types of modulations for physical communication between an ED and a gateway: The LoRa modulation and Gaussian frequency shift keying (GFSK). The former is commonly used, as its support is mandatory, whereas the latter is optional. LoRa uses chirp spread spectrum [21]. A LoRa symbol comprises 2^{SF} chips [22], where SF denotes the parameter called spreading factor. LoRaWAN defines 6 different SFs (called SF7 to SF12). Each SF leads to a different corresponding DR. For the sake of spectral efficiency, the SFs are orthogonal. In order to enhance link quality, LoRa also supports forward error correction by means of different coding rates (CRs), from 4/5 to 4/8.

LoRaWAN has been specified to operate in a number of world regions. In this article, we assume the LoRaWAN characteristics for Europe (EU). In this region, LoRaWAN uses the industrial, scientific, and medical (ISM) 868 MHz frequency band. Devices using this band must support the following three default radio channels: 868.1 MHz, 868.3 MHz, and 868.5 MHz. Different bit rates are possible, defined by the DR in use, which depend on the modulation, the SF and the channel bandwidth used [23]. DR0 to DR5 are mandatory, whereas DR6 and DR7 are optional. As a result, an EU LoRaWAN network typically offers bit rates between 250 bps and 5470 bps, which correspond to DR0 (SF12) and DR5 (SF7), respectively. In order to improve communication performance, pseudorandom frequency channel hopping is used.

Use of the unlicensed ISM 868 MHz band offers significant advantages in terms of operational cost. However, spectrum access in that band is regulated by ETSI, which establishes that if a listen-before-talk mechanism is not supported, then the uplink duty cycle must be lower than 1% for radio channel frequencies between 868.0 MHz and 868.6 MHz. In order to conform to such constraints, LoRaWAN enforces that an uplink sender must remain silent after a message transmission for a time interval of adequate duration.

In Class A, message transmission is initiated by the ED, as a way to allow this device to control when it needs to stay active or when it can return to sleep mode to save energy. Message transmission by the NS can only be performed in two specific time intervals called receive windows (RX1 and RX2) [10], which are opened after the ED has transmitted an uplink message. The start of RX1 and RX2 occurs after RECEIVE_DELAY1 and RECEIVE_DELAY2 (by default, 1 s and 2 s, respectively) after the ED transmission has finished. Message transmission by the NS requires a prior transmission by the ED to open a new receive window. By default, downlink transmission in RX1 is performed by using the same DR as the one used by the ED in its last transmission. In RX2, DR0 (i.e., SF12) is used by default, on the 869.525 MHz frequency channel [23]. This channel, which has been reserved for downlink use, is subject to a duty cycle restriction of less than 10% [24].

C. LoRaWAN MAC Layer

At the MAC layer, LoRaWAN provides an optional automatic repeat request (ARQ) mechanism, by which an ED can choose whether to request a positive acknowledgment (ACK) for each data frame to be transmitted. When an ACK is solicited (in which case the data frame is also known as a confirmed frame), the ACK needs to be received in either RX1 or RX2. If the ACK is not received, the ED retransmits the same frame, up to a maximum number of retries. In many deployed EDs [26], [27], the first two transmission attempts use the same DR and, subsequently, the next lower DR is used for the next two attempts (except if DR0 is used). However, this feature has been recently removed from the LoRaWAN specifications [28], [29], as it may degrade network performance [25]. Upon reaching the maximum number of transmission attempts for a given frame, the frame transmission is considered to have failed. Retransmissions are triggered by retransmission timer expiration. This timer is reset at the start of RX2 to a random value between 1 and 3 seconds, by default [23].

The LoRaWAN MAC also offers a mechanism called adaptive data rate (ADR), by which the NS manages ED parameters, such as the DR, the frequency channels, and the transmit power to be used, based on link quality estimates.

III. Related Work

Several papers have modeled the energy performance of LoRaWAN by means of mathematical analysis [6]–[10], [12]–[20], whereas a few others have studied it by using simulation [11], [18]. Impact of packet size on energy performance has only been considered in some of the analytical studies [10], [12]–[14], [17], [19]. The latter works are briefly reviewed next.

In [10], the energy cost of data delivery as a function of packet size was qualitatively captured for acknowledged transmissions. Curves following a "U" shape were obtained for different network loads, highlighting that there exists a medium packet size value that minimizes EPB. However, results were not quantified. In addition to its qualitative approach, the model is also limited by the fact that it does

not take into account duty cycle restrictions and it assumes that all traffic is confirmed.

EPB has been analytically modeled in the literature, for different frequency bands, and for different ranges of LoRaWAN packet sizes: Between 10 and 35 bytes [12], between 10 and 40 bytes [14], and between 1 and 51 bytes [13]. According to these works, EPB decreases monotonically with packet size, for different SFs and CRs. However, collisions and duty cycle restrictions were neglected. In [17], a similar analytical approach was followed, also overlooking collisions and duty cycle restrictions, and furthermore, only the LoRa layer of the LoRaWAN protocol stack (without specifying the coding and data rate) was considered. The work reports a monotonically decreasing lifetime as a function of packet size. A singular aspect of this work is that it evaluates packet sizes up to 1000 bytes, thus a large subset of the considered packet sizes are not valid.

Finally, the authors in [19] modeled EPB taking into account the number of EDs, the collision probability, the number of frame retransmissions and the duty cycle. However, only some packet size values were examined. As in the previously reviewed works, results exhibit an EPB decrease with packet size. In addition, it is shown that, due to collisions, an increase in the number of EDs or a more restrictive duty cycle can lead to an EPB increase. However, the model presents some serious drawbacks. First, duty cycle restrictions were only modeled for the ED, not for the gateway, thus the significant impact of the latter (Section IV) was not taken into account. Secondly, the traffic actually offered by the EDs was considered a Poisson process, which neglects the impact of the previously mentioned duty cycle restrictions on such traffic. Thirdly, according to the obtained results, EPB tends asymptotically to a finite value when the number of nodes increases; however, an EPB tending to infinity would be expected due to collisions preventing data from being successfully delivered (when the maximum number of retransmissions is exhausted), rendering the corresponding energy cost of data packet transmission (including retransmissions) useless. Finally, after two failed retransmissions, the DR is decremented. As mentioned in Section II.C, this behavior is no longer recommended [28], [29] and, in fact, its harmfulness has been proven [25].

From the analysis of the literature, we conclude that existing works are not sufficient to understand the impact of packet size on the LoRaWAN EPB in LoRaWAN.

IV. Energy Efficiency Evaluation

In this section, we present our comprehensive simulation study on the impact of packet size on the LoRaWAN EPB. We provide a detailed analysis and discuss the influence of several phenomena on the observed EPB behaviors.

The section is organized into three subsections. The first one provides the details of the simulation environment used and the scenarios that we have considered. In order to understand the limits on the achievable performance, the second subsection provides the evaluation results when all EDs work in confirmed transmission mode (CTM). Finally, in the third subsection, we consider mixed scenarios comprising both CTM EDs and EDs in unconfirmed transmission mode (UTM). We refer to CTM and UTM EDs as CEDs and UEDs, respectively.

A. Simulation Environment and Parameters

For the study, we use the OMNeT++ simulator with the AFLoRa framework, which we recently developed [25]. Based on the FLoRa framework v0.8 version [30], [31], AFLoRa adds support for the CTM (including the ACK and retransmission mechanisms). In a subsequent AFLoRa update that we purposefully designed for this paper, we also included functionality to support packets with different lengths, along with the corresponding computation of the duty cycle to conform with duty cycle regulations. As a side-contribution of the paper, we offer the new AFLoRa version publicly [32].

In all the scenarios simulated in this paper, there is a common set of parameters and settings, which are described in this paragraph. The simulated LoRaWAN network comprises one gateway, and several EDs. The gateway is placed in the center of a square region with a side of 142 m, whereas EDs follow a uniformly random spatial distribution within that region. The transmit power used by both the gateway and the EDs is 14 dBm. This is a sufficiently high transmit power level that ensures packet reception without losses due to link quality issues (either at EDs or at the gateway). This way, we can focus the study on congestion issues rather than losses due to insufficient link quality. Note that these conditions correspond to a well dimensioned network, and without unexpected scenario changes affecting radio propagation or interference conditions. Impact of lower quality links on performance is discussed in Section V.B. We also set the physical layer CR to 4/8, which corresponds to the highest protection against packet corruption, and we use the explicit header mode at the physical layer. Furthermore, the retransmission mechanism applied does not change the SF used after the first transmission attempt of a packet, and a maximum of 8 transmission attempts are performed. Finally, we consider a radio configuration as specified for the EU region. For each individual scenario, the total simulated time is 1 day.

In our evaluations, we take into account the impact of the SF used. More specifically, we consider SF7 and SF12, as the two edge values within the range of possible SFs. The physical transmission rates for SF7 and SF12 are fixed and equal to 5470 bps and 250 bps, respectively, regardless of the considered packet sizes. We consider several numbers of CEDs (denoted *NC*) and UEDs. The total number of EDs, including both CEDs and UEDs, is denoted *N*. Note that $NC \leq N$. We also evaluate different offered packet loads, where each ED aims to transmit packets by following a Poisson distribution with a mean time between packets of *TP* seconds. In our simulations, this distribution is shaped to fulfill the duty cycle restrictions.

The main performance parameter we focus on is EPB, which is obtained as the total energy cost of all the transmissions performed by EDs in the network divided by the total number of packet bits received successfully by the NS. We use the term "packet" to refer to the LoRaWAN frame payload. The energy cost computation is based on a published

LoRaWAN energy consumption model [10]. In the evaluation, we study the impact of packet size, within the range of valid maximum packet size values, on EPB, that is, 242 bytes for SF7 and 51 bytes for SF12 [23], when the MAC options field is not present (FOpts control field in [33]).

In order to understand the reasons behind the main performance parameter results, we also focus on the following network performance metrics: i) collision ratio (i.e., the number of MAC frames colliding at the gateway over the total number of MAC frames transmitted by EDs), ii) the gateway drop ratio due to duty cycle restrictions (i.e., the number of dropped MAC frames –actually, ACK frames– at the gateway over the total number of MAC frames transmitted by the NS to EDs), iii) the ED drop ratio (i.e., the number of dropped packets at EDs over the total number of packets to be transmitted), iv) the retransmission ratio at EDs (i.e., the number of frame retransmissions over the total number of frames transmitted by EDs), v) the packet delivery ratio (PDR) (i.e., the total number of packets delivered to the NS over the total number of packets generated by EDs), and vi) the number of delivered bits (NDB), (i.e., the number of packet bits delivered per packet generated by an ED).

B. CED-only Scenarios

1) EPB Results: We first evaluate EPB when all EDs are CEDs (i.e., $N = NC$). We consider different N values (100, 1000, and 2000), several ED loads, and the minimum and maximum SFs (i.e., SF7 and SF12). The results are depicted in Fig. 1, which are obtained for TP values of 4000 s (0.9 packet/h).

For SF7, and for low packet size values (up to ∼30 bytes), the EPB exhibits a dramatic decrease with packet size in all the considered cases (Fig. 1(a)). As packet size increases, frame transmission time also increases, as well as the related energy consumption. However, the physical and MAC frame header size, along with other energy-consuming LoRaWAN protocol and ED hardware overheads, remain constant, in contrast with packet size, producing the mentioned EPB decrease.

As packet size increases further, the EPB behavior depends on N. For $N = 100$ EDs, EPB decreases steadily with packet size. However, for $N = 1000$ and $N = 2000$, the EPB behavior changes, and it increases for the greater packet sizes considered. Therefore, in the latter cases, EPB presents an "asymmetric U" shape, and there exists a minimum value which is achieved for a medium, optimal packet size. This effect is more remarkable for low traffic loads and a high number of devices (Fig. 1(a)). The optimal packet size depends on traffic load and on the N value. For example, considering SF7, for $TP = 4000$ s and $N = 2000$ (Fig. 1(a)), the EPB minimum is achieved for a packet size of ∼100 bytes (Fig. 1(a)). We also evaluated other TP values. We found that, for $TP = 2000$ s and $N = 2000$, the minimum is found for a packet size of ∼51 bytes, whereas for $TP = 1000$ s and $N = 2000$, the optimal packet size is ∼40 bytes. These values show a tendency whereby the optimal packet size decreases as the offered load increases.

For SF12 (Fig. 1(b)), EPB is greater than that obtained for SF7, due to the greater transmission time. The latter also impacts other performance parameters, such as the number of collisions and frame drops, which further increase energy consumption. However, EPB decreases steadily with packet size within the range of valid packet sizes, and thus, it does not show the "U" shape found in some cases for SF7.

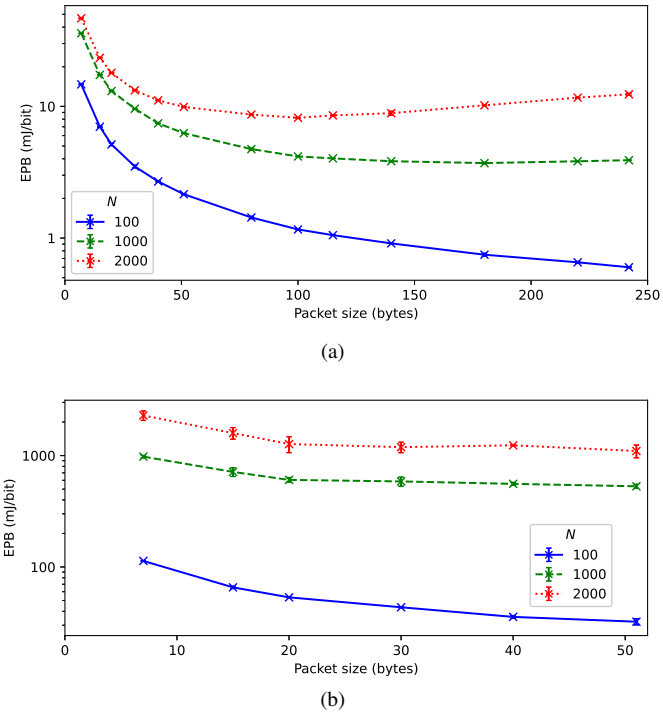

Fig. 1. EPB as a function of packet size for TP = 4000 s: (a) SF7, (b) SF12.

2) Understanding the EPB Results: In order to determine the reasons behind the obtained EPB results as a function of packet size, we next focus on the following additional performance parameters from the same evaluated scenarios: i) the frame retransmission ratio (Fig. 2), ii) PDR (Fig. 3), and iii) NDB (Fig. 4).

Note that EPB corresponds to a fraction where, for a given ED, the numerator is dominated by the retransmission ratio, and the denominator is equal to NDB. Therefore, in order to understand EPB behavior, it will be crucial to focus on the behavior of the retransmission ratio and NDB. The retransmission ratio depends on the collision ratio, ED drop ratio and gateway drop ratio, whereas NDB depends on PDR.

First, we analyze the performance for SF7, and N values of 1000 and 2000 (i.e., the SF and N values for which EPB as a function of packet size shows an "asymmetric U" shape), in terms of collision ratio, ED drop ratio, and gateway drop ratio.

For low packet sizes, the collision probability and ED drop ratio are relatively low, while the gateway drop ratio is high. The latter is due to the duty cycle restriction (i.e., 1% in the used frequency band in the downlink channel) and the high number of EDs (all of them being CEDs) that require ACKs in response. In consequence, there is a high number of unnecessary ED retransmissions (Fig. 2(a)) that leads to a high EPB, and also due to the low packet size itself.

When packet size increases, initially, EPB decreases due

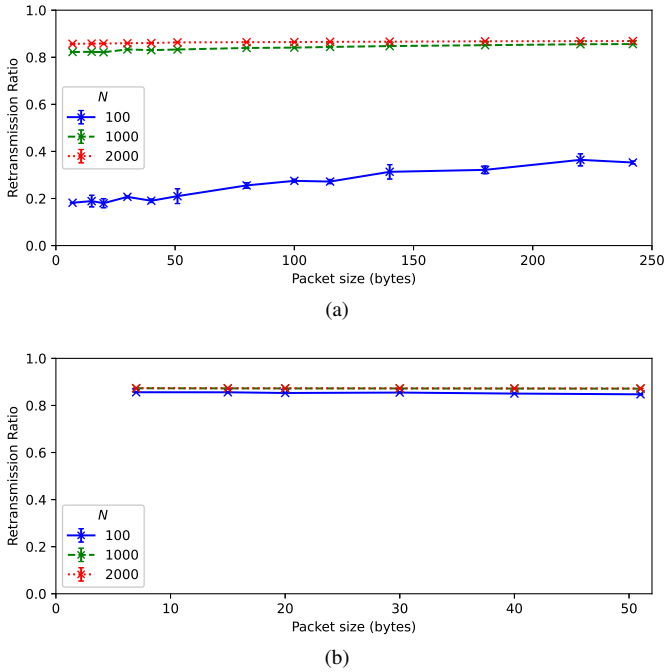

Fig. 2. Retransmission ratio from EDs for $TP = 4000$ s: (a) SF7, (b) SF12.

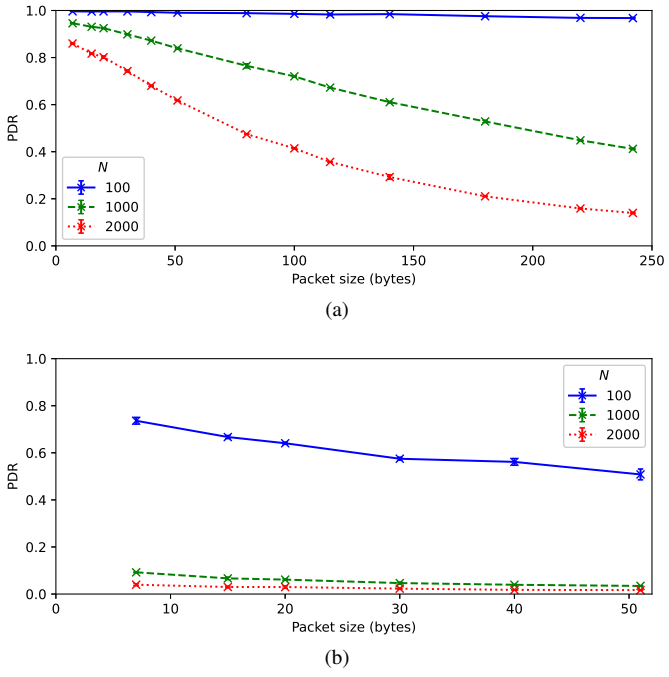

Fig. 3. PDR for $TP = 4000$ s: (a) SF7, (b) SF12.

to the dominant effect of a greater amount of delivered bits over the energy overheads that are independent of packet size. However, the collision ratio increases quickly, and the ED drop ratio also increases; in consequence, the gateway drop ratio decreases, since the NS receives a lower number of frames, and therefore it sends a lower number of ACKs in response to the EDs. For high packet sizes, ED retransmissions (Fig. 2(a)) slightly increase (from an already high amount for low packet sizes) due to the very high collision ratio and ED drop ratio. PDR decreases significantly with packet size (Fig. 3(a)), in

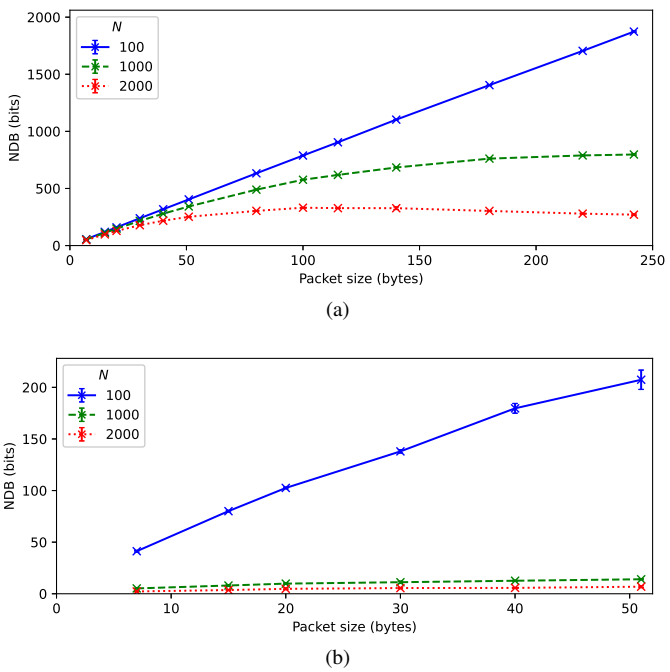

Fig. 4. NDB for $TP = 4000$ s: (a) SF7, (b) SF12.

such a way that NDB initially increases, reaches a maximum, and finally decreases with packet size (Fig. 4(a)). The relatively constant retransmission ratio with packet size leads to EPB being mostly dominated by the inverse of NDB, thus producing the "asymmetric U" shape shown previously in Fig. 1(a) for SF7 and $N = 1000, 2000$. In contrast, for SF12, and for the same N values, there is a higher collision ratio and ED drop ratio not only for high packet sizes, but also for low ones. The collision ratio is close to 1, due to the high frame transmission time for SF12 and the high number of EDs competing for transmission resources. The high collision and ED drop ratios, combined with a decreasing gateway drop ratio lead to a relatively constant number of retransmissions (Fig. 2(b)), which combined with an almost constant PDR (Fig. 3(b)) and a linearly increasing NDB with packet size (Fig. 4(b)), yield a monotonically decreasing EPB with packet size (Fig. 1(b)).

For SF7 and $N = 100$, as illustrated in Fig. 1(a)), EPB decreases monotonically with packet size. This occurs because, in this scenario, the lower amount of EDs produces lower offered traffic load. While the collision ratio and the ED drop ratio increase with packet size, they remain low (compared to those obtained for greater N values). Note that, in consequence, the gateway drop ratio and the retransmission ratio remain low and near-independent of packet size (Fig. 2(a)), whereas PDR is high, exhibiting only a slight decrease with packet size (Fig. 3(a)), thus NDB increases linearly with packet size (Fig. 4(a)). As a result, EPB decreases inversely with packet size (Fig. 1(a)). For SF12 and $N = 100$, the retransmission ratio is very high and constant with packet size (Fig. 2(b)). On the other hand, PDR is already moderately high for low packet sizes and it decreases only slightly with packet size (Fig. 3(b)), therefore NDB increases almost linearly with packet size (Fig. 4(b)). In consequence, EPB

decreases monotonically with packet size (Fig. 1(b)).

Note that, for SF7, the retransmission ratio is between 82.1% and 87.3% (Fig. 2(a)), for $N \geq 1000$ and for all packet sizes considered, which means that a large subset of the transmissions are retransmissions, and reflects that the system is saturated. This is consistent with the fact that, in the worst case, for each packet to be transmitted, there is one first attempt and 7 frame retransmissions, which leads to an upper bound for the retransmission ratio of 87.5%. This is also the case for SF12 and all the considered *N* values, where the retransmission ratio is around 87.4% (Fig. 2(b)).

C. Mixed CED and UED Scenarios

In this subsection, we evaluate mixed scenarios with *NC* CEDs, and $N-NC$ UEDs. Our aim is to study EPB behavior in scenarios where at least a subset of the EDs (i.e., the UEDs) do not perform retransmissions.

We analyze two main cases: $NC = 100$ and $NC = 1000$, for different *N* values. For all of them, we consider SF7, SF12, and $TP = 4000$ s.

Fig. 5(a) shows EPB as a function of packet size for $NC = 100$, for SF7, and for different *N* values. EPB decreases dramatically with packet size, even for high numbers of UEDs. This occurs because the low offered load produces a relatively low collision ratio, a low ED drop ratio, and a low gateway drop ratio due to duty cycle constraints. The retransmission ratio of CEDs slightly increases with packet size (Fig. 6(a)), whereas UEDs perform a single transmission attempt for each packet to be sent. For CEDs, PDR is very high and almost constant with packet size (Fig. 7(a)), whereas for UEDs, PDR decreases to a greater extent with packet size, as expected (Fig. 7(b)). In consequence, for CEDs, NDB increases linearly with packet size (Fig. 8(a)), whereas for UEDs, NDB increases with packet size less than for CEDs, but still increases monotonically with packet size (Fig. 8(b)). In consequence, for $NC = 100$, EPB decreases monotonically with packet size (Fig. 5(a)).

In contrast, for $NC = 1000$, SF7 and different values of *N* (Fig. 9(a)), a different behavior can be observed, with a slight EPB increase for high packet size and high *N* values, which produces "asymmetric U" shape curves with packet size. The collision ratio increases significantly with packet size, even exceeding 80%, due to the high number of EDs (from $N = 1000$ to $N = 5000$) and because a significant part of them ($NC = 1000$) use CTM. The ED drop ratio is low (below 10%), due to the relatively low load for each ED of a packet transmission every 4000 s, and the low transmission times due to SF7, in relation to duty cycle limitations. The gateway drop ratio decreases with packet size because a lower number of ACK frames need to be transmitted by the NS (due to a lower number of uplink frames reaching it). As packet size increases, the greater number of collisions slightly increases the already high retransmission ratio of CEDs, ranging from 82.2% for the smallest packet size, up to 86.3% for the greatest one. PDR decreases significantly with packet size for both CEDs and UEDs (Figs. 10(a) and 10(b), respectively), which leads to an NDB significant increase with packet size only

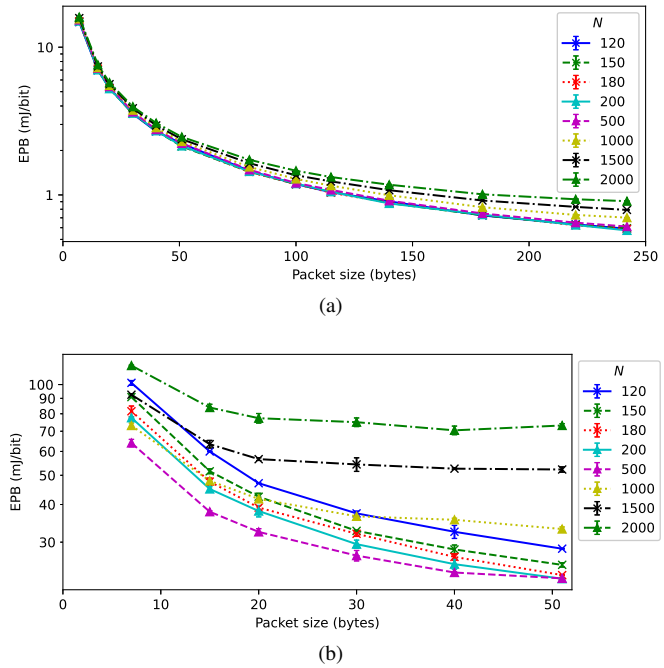

Fig. 5. EPB as a function of packet size for $TP = 4000$ s, $NC = 100$, and several *N* values: (a) SF7, (b) SF12.

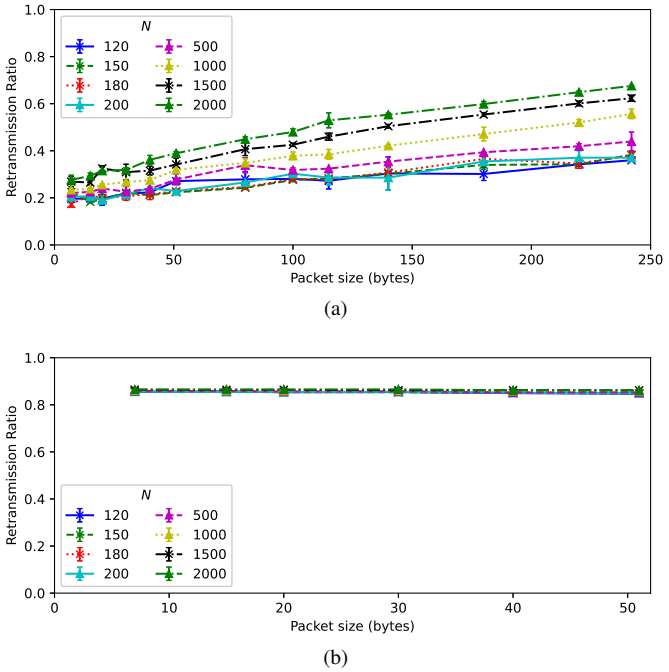

Fig. 6. Retransmission ratio from EDs for $TP = 4000$ s, $NC = 100$, and several *N* values: (a) SF7, (b) SF12.

for low packet size (Figs. 11(a) and 11(b), respectively). As packet size increases further, NDB reaches a maximum value and then decreases (the maximum NDB is found for a packet size that decreases with *N*, since PDR also decreases with *N*). In consequence, EPB follows a behavior inverse to the NDB one with packet size, adopting an "asymmetric U" shape.

When SF12 is used (Figs. 5(b) and 9(b)), EPB is greater than for SF7 as expected, due to the greater transmission time. For $NC = 100$ and $N = 2000$ (Fig. 5(b)), EPB follows

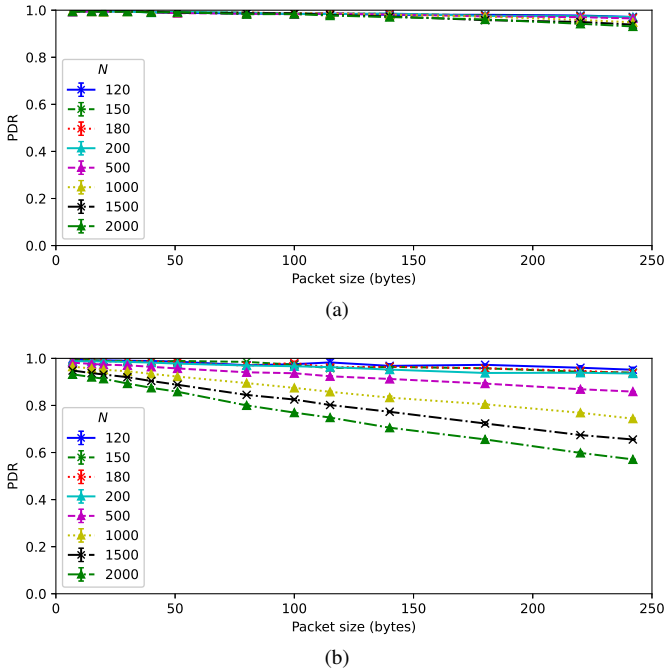

(a) (b)

Fig. 7. PDR for $TP = 4000$ s, $NC = 100$, SF7, and several N values: (a) CEDs, (b) UEDs.

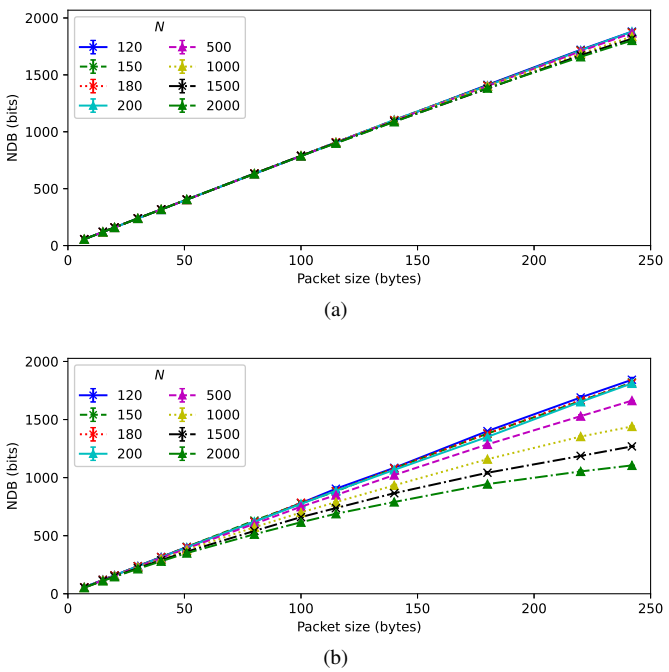

(a) (b)

Fig. 8. NDB for $TP = 4000$ s, $NC = 100$, SF7, and several N values: (a) CEDs, (b) UEDs.

an "asymmetric U" shape, with an optimal packet size (that minimizes EPB) of ∼40 bytes. While the collision ratio is moderate for lower N values, it increases significantly with N. The ED drop ratio is greater than that obtained for SF7, due to the greater transmission time of SF12. In consequence, for CEDs, the retransmission ratio is close to its maximum value and constant with N (Fig. 6(b)), due to the large transmission time for SF12. PDR tends to slightly decrease with packet size and with N (Fig. 12). As a result, NDB increases with packet size linearly for low N , but as N increases, NDB flattens (Fig. 13), becoming almost constant with packet size for $N = 2000$, which produces the slight "asymmetric U" EPB shape that can be observed for this value of N in Fig. 5(b).

For SF12 and $NC = 1000$, EPB tends to decrease with packet size (Fig. 9(b)). The high number of nodes and high transmission time due SF12 produce a very high and almost constant collision ratio. This reduces the amount of ACK frames to be transmitted to EDs from the NS, which are less affected by duty cycle restrictions at the gateway. In consequence, the gateway drop ratio is similar to the one for SF7 and $NC = 1000$. For SF12, ED packet drops show greater values than for SF7, due to the greater transmission time of the former. The high collision ratio and relatively high ED drop ratio lead to very high and almost constant CED retransmission ratio, of ∼87.2% for all packet sizes and scenarios considered, and very low PDR (which is constant with packet size). For CEDs, PDR ranges between 9.1% and 5.9% for the smallest packet size, and between 3.6% and 2.6% for the greatest one. For UEDs, PDR follows a similar behavior, with a maximum value of 6%, which is obtained for the smallest packet size. This yields an NDB that increases linearly with packet size (Fig. 14). In consequence, EPB decreases inversely with packet size.

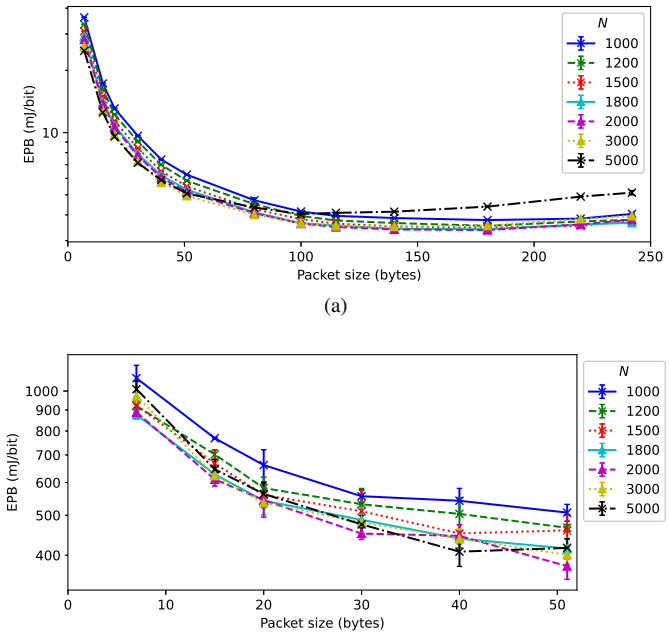

(a) (b)

Fig. 9. EPB as a function of packet size for $TP = 4000$ s, $NC = 1000$, and several N values: (a) SF7, (b) SF12.

V. Discussion

In this section, we first summarize the main observations from the evaluation performed in the previous section. Then, we discuss the impact of further parameters and scenarios on the network performance parameters considered in the previous section, along with an additional performance parameter such as packet delay.

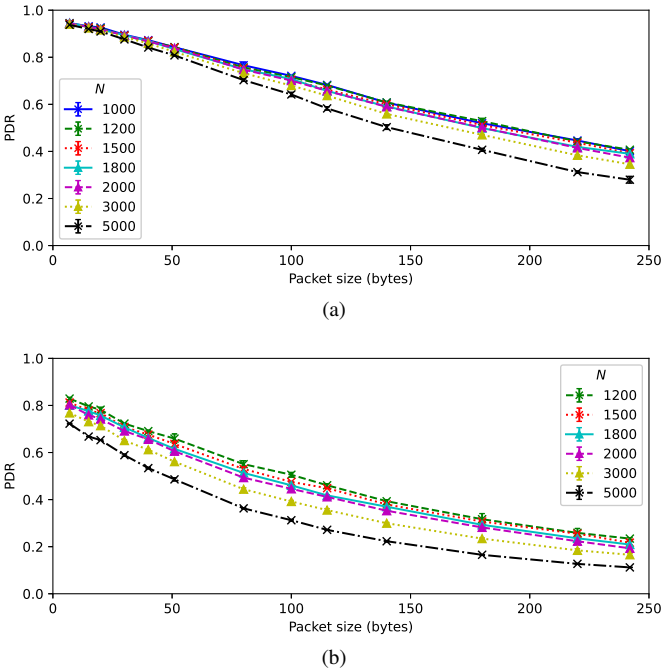

(a)

(b)

Fig. 10. PDR for $TP = 4000$ s, $NC = 1000$, SF7, and several N values: (a) CEDs, (b) UEDs.

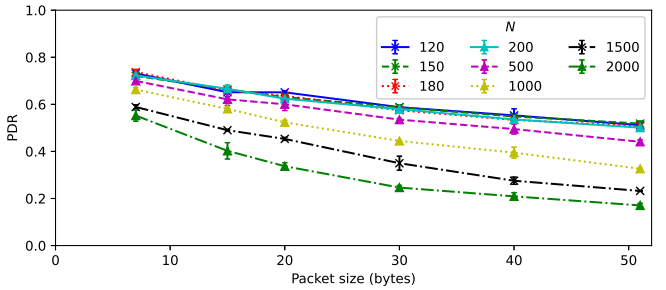

(a)

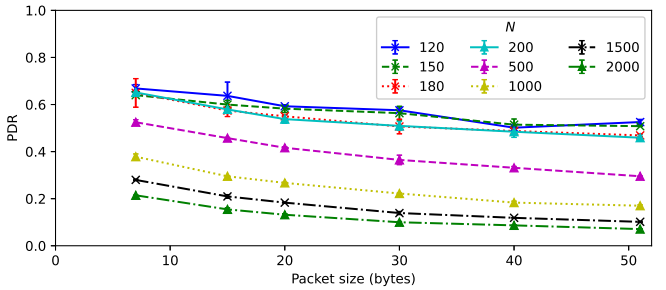

(b)

Fig. 12. PDR for $TP = 4000$ s, $NC = 100$, SF12, and several N values: (a) CEDs, (b) UEDs.

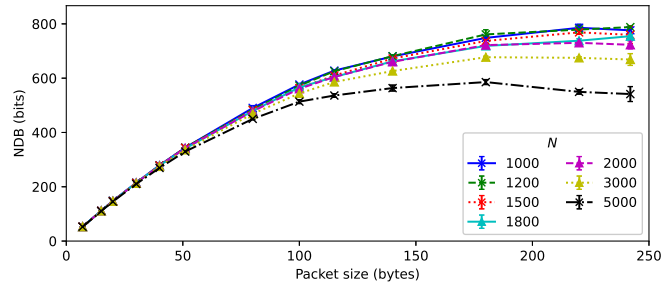

(a)

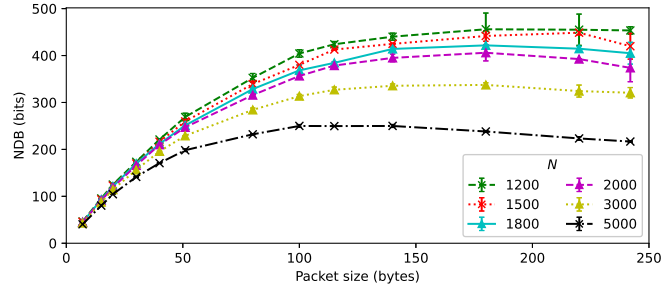

(b)

Fig. 11. NDB for $TP = 4000$ s, $NC = 1000$, SF7, and several N values: (a) CEDs, (b) UEDs.

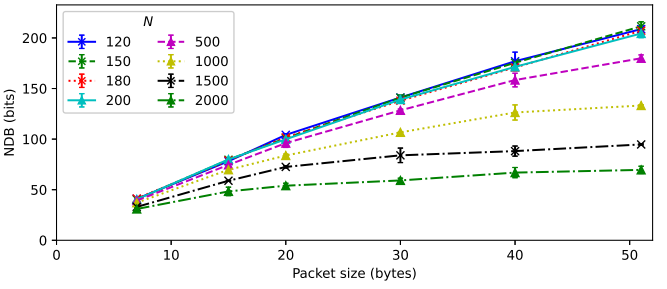

(a)

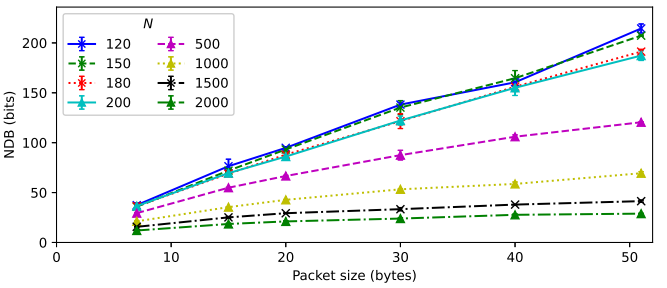

(b)

Fig. 13. NDB for $TP = 4000$ s, $NC = 100$, SF12, and several N values: (a) CEDs, (b) UEDs.

A. Summary of Observations

In a given scenario, the offered network load (which increases with N, NC, and SF, and decreases with *TP*) determines the behavior of the scenario in terms of ED drop ratio, collision ratio and gateway drop ratio. These parameters in turn determine the main performance parameters used in our analysis in Section IV, that is: i) CED retransmission ratio, ii) PDR, and iii) NDB. As explained in Section IV.B.2, EPB can be understood as a fraction where the numerator is dominated by the retransmission ratio, and the denominator is the NDB.

Tables I and II provide a summary of the main performance results and observations from Sections IV.B and IV.C, that is, CED-only and mixed CED and UED scenarios, respectively. We next extract a general behavior from such evaluation results.

For low or high offered network loads, the retransmission ratio generally remains rather constant with packet size, and at low or high values, respectively. In consequence, the PDR

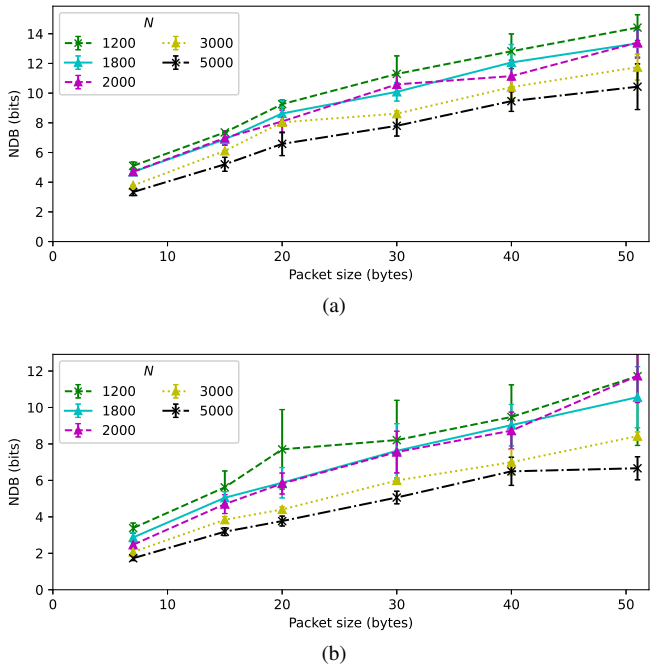

Fig. 14. NDB for $TP = 4000$ s, $NC = 1000$, SF12, and several N values: (a) CEDs, (b) UEDs.

TABLE I
SUMMARY OF PERFORMANCE RESULTS AND OBSERVATIONS: CED-ONLY SCENARIOS.

	$NC = 100$		$NC = 1000$	
	SF7	SF12	SF7	SF12
RR	Low, slight increase	Very high, ∼constant	Very high, ∼constant	Very high, constant
PDR	Very high, ∼constant	High, slight decrease	Significant decrease	Very low, ∼constant
NDB	Linear increase	Linear increase	Flattens, "inverse U"	Very low, linear increase
EPB	Decrease	Decrease	"Asymmetric U"	Decrease

The attributes in the table refer to the behavior of each corresponding performance parameter (retransmission ratio (RR), PDR, NDB, or EPB) as a function of packet size.

is also rather constant with packet size. Such PDR behavior leads to an NDB increase with packet size that produces an EPB decrease with packet size. In such cases, the packet size that minimizes EPB is the largest one supported for the SF being used.

However, under medium offered network loads, even if the retransmission ratio remains high and constant with packet size, PDR decreases significantly with packet size, therefore NDB does not monotonically increase with packet size and even decreases for high packet sizes. In such conditions, EPB exhibits an "asymmetric U" shape with packet size, with an optimal packet size, of a medium value, that minimizes EPB.

In our evaluated scenarios, EPB follows an "asymmetric U" shape in the following cases: i) in CTM-only scenarios, for $N \geq 1000$ and SF7, ii) in mixed scenarios, for $NC = 100$, $N = 2000$ and SF12, and iii) in mixed scenarios, for $NC = 1000$ and SF7. Otherwise, the optimal packet size is the greatest one allowed for the SF used.

TABLE II
SUMMARY OF PERFORMANCE RESULTS AND OBSERVATIONS: MIXED CED AND UED SCENARIOS.

	$NC = 100$		$NC = 1000$	
	SF7	SF12	SF7	SF12
RR (for CEDs)	Linear increase	Very high, constant	Very high, ∼constant	Very high, constant
PDR (for CEDs)	Very high, ∼constant	Linear decrease (significant for high N)	Significant decrease	Very low, ∼constant
PDR (for UEDs)	High, linear decrease	Linear decrease (significant for high N)	Significant decrease	Very low, ∼constant
NDB (for CEDs)	Linear increase	Linear increase (flattens for high N)	Flattens to "inverse U"	Linear increase
NDB (for UEDs)	Linear increase (flattens with N)	Linear increase (flattens for high N)	Flattens to "inverse U"	Linear increase
EPB	Decrease	"Asymmetric U" (for high N)	"Asymmetric U"	Decrease

The attributes in the table refer to the behavior of each corresponding performance parameter (RR, PDR, NDB, or EPB) as a function of packet size.

B. Impact of the Received Signal Power on Performance

The evaluation carried out in Section IV uses a sufficiently high transmit power level that ensures packet reception without losses due to link quality issues.

However, if the network is not well dimensioned, and/or the environment suffers unexpected changes affecting radio propagation and/or interference conditions, losses due to bit errors may occur. Such losses would contribute to producing or emphasizing a U-shaped EPB as a function of packet size, with an increasing EPB for the greater packet sizes: the probability of packet loss due to bit errors would increase with packet size, potentially increasing the retransmission ratio (for CEDs), and/or decreasing NDB, with packet size.

C. Impact of the Network Topology on Performance

In Section IV, the considered scenarios comprise a single gateway. However, LoRaWAN deployments may offer connectivity to EDs via more than one gateway. In a multigateway scenario, even under homogeneous and equivalent network traffic conditions, an ED may have greater opportunities for successful data packet delivery, thus increasing NDB (and, for a CED, also reducing its retransmission ratio, not only due to a lower overall collision probability, but also because of the possibility to balance ACK traffic across the existing gateways, offering chances to reduce gateway ACK drops [34]). Therefore, we expect the U-shaped EPB curve versus packet size observed in some of the single-gateway scenarios in Section IV to become less steep on its right side, even leading to a

strictly decreasing curve versus packet size when performance is significantly improved. Equivalently, network offered load would need to be greater to produce a U-shaped curve.

D. Packet Delay

While this paper focuses on EPB as primary performance parameter, packet delay is another interesting performance parameter in the context of the scenarios considered in this work. In order to understand packet delay performance, we can identify two relevant device categories: CEDs and UEDs.

CEDs will retransmit a packet in absence of a corresponding ACK. Such event may be due to packet collisions, which will contribute to increasing packet delay. However, a subset of retransmissions are unnecessary and do not incur additional packet delay (although they may increase the network congestion level and thus affect other packet transmissions), since in some cases packets are correctly delivered, but their corresponding ACKs are dropped by the gateway. For SF7, the maximum delay for a packet transmitted by a CED, as a function of the number of retransmissions (denoted N_{rtx}), is $\sim 0.63 + 62.7 N_{rtx}$ seconds. For SF12, such maximum delay is $\sim 4.0 + 407 N_{rtx}$ seconds. Note that an additional backbone delay would need to be added.

UEDs do not perform retransmissions, therefore their packet delay is bounded (assuming a backbone network with a bounded delay). For SF7 and SF12, the maximum theoretical delay is 626.94 ms and 4071.42 ms, respectively, plus the backbone network delay.

LoRaWAN is often used as a technology for packet transmission without strict delay requirements [1]. The increased delays incurred by CEDs due to packet retransmission are compatible with delay-tolerant applications. However, use of SF7 offers significantly lower latency for UEDs or for CEDs under low offered load, albeit not achieving real-time performance.

VI. Conclusions

In this paper we have studied the energy efficiency of LoRaWAN as a function of packet size. We have conducted extensive simulations, using OMNeT++ with the AFLoRa framework, in order to evaluate the EPB of a LoRaWAN device. In addition to the packet size, we have considered the impact of the SF, the number of CEDs and UEDs, and the offered packet load on EPB.

We have found that, in very low or very high offered traffic load scenarios, the most energy-efficient packet size is the largest one supported for the SF being used. As the offered traffic load deviates from the two extreme conditions mentioned, a shorter packet size may minimize EPB. In general, the curve that depicts EPB as a function of packet size exhibits an "asymmetric U" shape. A very small packet size incurs high energy overhead per delivered data bit, whereas a large packet size increases the probability of collision and ED drops (and, for CEDs, the number of retransmissions too). While PDR tends to decrease with packet size, it remains almost constant, thus NDB increases monotonically with packet size, for very low or very high offered traffic, respectively. In such cases, the rightmost side of the "U" shape is not visible for the range of LoRaWAN valid packet sizes. Otherwise, PDR may decrease significantly with packet size and NDB may adopt an "inverse U" shape with packet size, in turn producing an "asymmetric U" shape for EPB.

In our considered scenarios, the "asymmetric U" shape falls within valid packet sizes in the following cases: i) in CED-only scenarios, for SF7 and $N \geq 1000$, ii) in mixed scenarios, for SF7 and $NC = 1000$ (for all N values considered), and iii) in mixed scenarios, for SF12, $NC = 100$, and $N = 2000$. In such cases, using the EPB-optimal packet size decreases EPB by up to 34% compared with using the greatest corresponding valid packet size.

We believe that our results will be useful for developers, researchers, engineers, network operators and practitioners in the field of LoRaWAN networks.

References

[1] J. Haxhibeqiri, E. De Poorter, I. Moerman, and J. Hoebeke, "A survey of LoRaWAN for IoT: From technology to application," *Sensors*, vol. 18, no. 11, p. 3995, 2018.

[2] M. A. Ertürk, M. A. Aydın, M. T. Büyükakkaşlar, and H. Evirgen, "A survey on LoRaWAN architecture, protocol and technologies," *Future Internet*, vol. 11, no. 10, p. 216, 2019.

[3] M. A. M. Almuhaya, W. A. Jabbar, N. Sulaiman, and S. Abdulmalek, "A survey on LoRaWAN technology: Recent trends, opportunities, simulation tools and future directions," *Electronics*, vol. 11, no. 1, p. 164, 2022.

[4] P. Hofmann, Y. Schmitz, B. Quink, M. Parsa, and J. Olejak, "Comparison and analysis of security aspects of LoRaWAN and NB-IoT," *Deutsche Telekom IoT*, 2021.

[5] C. Bormann, M. Ersue, A. Keranen, and C. Gomez, "Terminology for constrained-node networks", *IETF Internet Draft, draft-ietf-lwig-7228bis-00*, 2022.

[6] B. Kim and K. Hwang, "Cooperative downlink listening for low-power long-range wide-area network," *Sustainability*, vol. 9, no. 4, 2017.

[7] G. Conus, G. Lilis, N. A. Zanjani, and M. Kayal, "An event-driven low power electronics for loads metering and control in smart buildings," in *Proc. EBCCSP*, 2016.

[8] D. Sartori and D. Brunelli, "A smart sensor for precision agriculture powered by microbial fuel cells," in *Proc. IEEE SAS*, 2016.

[9] J. Toussaint, N. El Rachkidy, and A. Guitton, "Performance analysis of the on-the-air activation in LoRaWAN," in *Proc. IEEE IEMCON*, 2016.

[10] L. Casals, B. Mir, R. Vidal, and C. Gomez, "Modeling the energy performance of LoRaWAN," *Sensors*, vol. 17, no. 10, p. 2364, 2017.

[11] J. Finnegan, S. Brown, and R. Farrell, "Modeling the energy consumption of LoRaWAN in ns-3 based on real world measurements," in *Proc. GIIS*, 2018.

[12] T. Bouguera, J. -F. Diouris, J. -J. Chaillout, and G. Andrieux, "Energy consumption modeling for communicating sensors using LoRa technology," in *Proc. IEEE CAMA*, 2018.

[13] R. Eriksen, "Energy consumption of low power wide area network node devices in the industrial, scientific and medical band", *Dissertation*, 2019.

[14] N. Pukrongta and B. Kumkhet, "The relation of LoRaWAN efficiency with energy consumption of sensor node," in *Proc. ICPEI*, 2019.

[15] R. K. Singh, P. P. Puluckul, R. Berkvens, and M. Weyn, "Energy consumption analysis of LPWAN technologies and lifetime estimation for IoT application," *Sensors*, vol. 20, no. 17, p. 4794, 2020.

[16] H. H. R. Sherazi, L. A. Grieco, M. A. Imran, and G. Boggia, "Energy-efficient LoRaWAN for industry 4.0 applications," in *IEEE Trans. Ind. Informat.*, vol. 17, no. 2, pp. 891–902, 2021.

[17] M. K. Nurgaliyev, A. K. Saymbetov, B. N. Zholamanov, A. T. Yeralkhanova, and G. B. Zhuman, "Predicting the lifetime of LoRa based wireless sensor networks using a probabilistic model of Markov chains," *News of NAN RK. SGTS*, vol. 2, no. 336, pp. 157–164, 2021.

[18] R. Marini, K. Mikhaylov, G. Pasolini, and C. Buratti, "LoRaWANSim: A flexible simulator for LoRaWAN networks," *Sensors*, vol. 21, no. 3, p. 695, 2021.
[19] S. Maudet, G. Andrieux, R. Chevillon, and J.-F. Diouris, "Refined node energy consumption modeling in a LoRaWAN network," *Sensors*, vol. 21, no. 19, p. 6398, 2021.
[20] H. Taleb, A. Nasser, G. Andrieux, N. Charara, and E. M. Cruz, "Energy consumption improvement of a healthcare monitoring system: Application to LoRaWAN," *IEEE Sensors J.*, vol. 22, no. 7, pp. 7288–7299, 2022.
[21] Semtech Corporation. "SX1272/3/6/7/8: LoRaModem. Designer's Guide. AN1200.13", Semtech Corporation: Camarillo, CA, USA, 2013.
[22] A. Augustin, J. Yi, T. Clausen, and W. M. Townsley, "A study of LoRa: Long range & low power networks for the Internet of things," *Sensors*, vol. 16, p. 1466, 2016.
[23] RP002-1.0.2 LoRaWAN™ Regional Parameters, LoRa Alliance Technical Committee: Fremont, CA, USA, 2020.
[24] ETSI EN 300.220-2 v3.2.1 (2018-06), "Short range devices (SRD) operating in the frequency range 25 MHz to 1000 MHz. part 2: Harmonised standard for access to radio spectrum for non specific radio equipment". Accessed: Dec. 30, 2022. [Online]. Available: https://www.etsi.org/deliver/etsi_en/300200_300299/30022002/03.02.01_60/en_30022002v030201p.pdf
[25] L. Casals, C. Gomez, and R. Vidal, "The SF12 well in LoRaWAN: Problem and end-device-based solutions," *Sensors*, vol. 21, no. 19, p. 6478, 2021.
[26] LoRa Alliance Technical Committee, "LoRaWAN specification", Version V1.0.3, LoRa Alliance: Beaverton, OR, USA, 2018.
[27] LoRa Alliance Certification. Accessed: Dec. 30, 2022. [Online]. Available: https://lora-alliance.org/lorawan-certification
[28] A. Yegin and O. Seller, "LoRaWAN® L2 1.0.4 Specification (TS001-1.0.4)", LoRa Alliance, 2020.
[29] N. Sornin and A. Yegin, "LoRaWAN® 1.1 Specification", LoRa Alliance, 2017.
[30] FLoRa. Framework for LoRa. Accessed: Dec. 30, 2022. [Online]. Available: https://flora.aalto.fi
[31] M. Slabicki, G. Premsankar, and M. Di Francesco, "Adaptive configuration of LoRa networks for dense IoT deployments," in *Proc. IEEE/IFIP NOMS*, 2018.
[32] AFLoRa v1. Accessed: Dec. 30, 2022. [Online]. Available: https://github.com/lluiscas/AFLoRa-v1
[33] LoRaWAN® Regional Parameters RP002-1.0.4, LoRa Alliance, 2022
[34] V. Di Vincenzo, M. Heusse, and B. Tourancheau, "Improving downlink scalability in LoRaWAN," in *Proc. IEEE ICC*, 2019.

Lluís Casals received his M.Sc. and PhD. degrees from Universitat Politècnica de Catalunya (UPC) in 1998 and 2023, respectively.

He is an Associate Professor at the same university. He has worked in several publicly funded research projects, and is co-author of several papers published in journals. His current research interests include energy efficiency of wireless sensor networks, low-power wide-area networks and the Internet of Things.

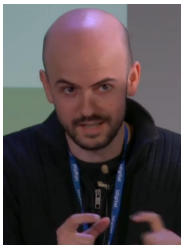

Carles Gomez received his PhD. degree from Universitat Politècnica de Catalunya (UPC) in 2007.

He is a Full Professor at the same university. He is a co-author of numerous technical contributions including papers published in journals and conferences, IETF RFCs, and books. His current research interests focus mainly on the Internet of things.

Dr. Gomez serves as an Editorial Board Member of several journals. He is also an IETF 6Lo Working Group Chair.

Rafael Vidal received his M.Sc. and PhD. degrees from Universitat Politècnica de Catalunya (UPC) in 1997 and 2007, respectively.

He is an Associate Professor at the same university. He has worked in several publicly funded research projects, and is co-author of several papers published in journals and conferences. His current research interests include performance of wireless networks (in particular, low-power wide-area networks) and the Internet of things.